Composite Structures 95 (2013) 539–546

Contents lists available at SciVerse ScienceDirect

Composite Structures

journal homepage: www.elsevier.com/locate/compstruct

Flutter analysis of composite lifting surfaces by the 1D Carrera Unified Formulation and the doublet lattice method

M. Petrolo *

Department of Mechanical and Aerospace Engineering, Politecnico di Torino, Corso Duca degli Abruzzi 24, 10129 Torino, Italy.

ARTICLE INFO

Article history:
Available online 9 July 2012

Keywords:
Unified formulation
Beam
Doublet lattice method
g-Method
Flutter

ABSTRACT

Flutter analyses of composite lifting surfaces are presented in this paper. Results were obtained through an advanced aeroelastic formulation based on higher-order 1D structural models coupled with the doublet lattice method. The *g*-method was used to compute flutter conditions. The Carrera Unified Formulation (CUF) was exploited to build 1D structural models. Refined theories were obtained by using Taylor-like expansions of the cross-section displacement field. In the CUF framework, the order (N) of the expansion is considered as a free-parameter, this means that N can be considered as an input of the analysis. Convergence studies on N can be straightforwardly conducted in order to establish the proper 1D theory for a given problem. Flutter analyses were conducted on several structural configurations. The effect of the stacking sequence and the effect of the sweep angle were analyzed. Results show the enhanced capabilities of CUF 1D in dealing with the flutter analysis of typical composite lifting surfaces with plate-like accuracy and low computational costs.

1. Introduction

Flutter is a dynamic phenomenon due to fluid–structure interactions. Typically, flutter can occur to aircraft structures, blades and bridges. Flutter must be avoided since it consists of undamped vibrations which can lead to catastrophic collapses. Different analysis tools have been developed over the last decades to predict flutter [1,2]. Amongst them, the doublet lattice method (DLM) emerged as one of the most powerful technique for flutter predictions. DLM was first developed in late 1960s [3]; more recently, an improved version of DLM has been proposed by Rodden [4]; this last version is the one utilized in this work. Three main features are responsible of DLM's success [1]:

1. It offers good accuracy (unless transonic regimes are considered and/or separation occurs).
2. DLM is cost competitive with respect to simpler methods such as strip theories.
3. Fairly complex geometries can be analyzed.

In this paper, DLM was coupled with a 1D structural refined formulation. 1D structural models – commonly referred to as beam models – are extensively used to analyze the structural behavior of slender bodies, such as columns, arches, blades, aircraft wings and bridges. In a 1D model, the 3D problem is reduced to a set of variables that only depends on the beam-axis coordinate. 1D structural elements are simpler and computationally more efficient than 2D (plate/shell) and 3D (solid) elements. This feature makes beam theories still very attractive for the static, dynamic and aeroelastic analysis of structures.

The classical beam theories are those by Euler–Bernoulli [5,6] and Timoshenko [7]. None of these theories can detect non-classical effects such as warping, out- and in-plane deformations, torsion-bending coupling or localized boundary conditions (geometrical or mechanical). These effects are important when, for instance, small slenderness ratios, thin walls and the anisotropy of the materials are considered. An accurate aeroelastic analysis requires the proper detection of non-classical effects.

Composite lifting surfaces were considered in this paper. The use of composite materials is advantageous for many reasons, such as high strength-to-weight ratio, high stiffness-to-weight ratio, ease of formability, wide range of operating temperatures and their capability to be tailored according to a given requirement, see the book by Tsai [8]. Tailoring is, in particular, extremely important for aeroelastic applications where composites are exploited to clear lifting surfaces of flutter or divergence. Typical composite materials have low transverse shear moduli compared to the axial tensile moduli. As a consequence, the related structures show higher transverse shear deformability compared to homogeneous isotropic materials, being this aspect a critical one in terms of modeling strategies and accuracy.

* Tel.: +39 011 090 6869; fax: +39 011 090 6899.
E-mail address: marco.petrolo@polito.it

0263-8223/$ - see front matter © 2012 Elsevier Ltd. All rights reserved.
http://dx.doi.org/10.1016/j.compstruct.2012.06.021

Many refined beam models have been developed over the last decades for the analysis of composite structures. Excellent reviews on these models are those by Kapania and Raciti [9] and Reddy [10]. Different classes of refined beam models were developed and, amongst them, the following are cited: the introduction of shear correction factors, the use of warping functions and De Saint–Venant's solution, asymptotic methods, Generalized Beam Theories (GBTs) and higher-order beam models. Some of the most relevant contributions are discussed below, with particular attention being given to the analysis of composite beam structures, which is the main task of the present paper.

Shear correction factors [11–14] and warping functions [15,16] are usually exploited to improve the global response of classical beam theories. The De Saint–Venant solution has represented the theoretical framework of many advanced beam models, as in the works by Ladeveze and co-workers, where the 3D elasticity equations were reduced to beam-like structures [17]. Asymptotic methods exploit an asymptotic expansion of a characteristic parameter, such as the thickness of the beam, to build refined theories, as in the seminal paper by Berdichevsky et al. [18]. Some valuable contributions on asymptotic methods are those related to VABS [19–21]. The key feature of this methodology is that the 1D model is governed by variationally consistent and geometrically exact governing equations which provide asymptotically exact stress and strain recovery by means of a beam model having a low number of degrees of freedom. Regular and thin-walled beams can be accounted for. The Generalized Beam Theory (GBT) was introduced by Schardt [22]. In the GBT framework, the cross-section displacement field of a thin-walled beam is assumed as a linear combination of deformation modes defined on a number of cross-section nodes. The proper choice of the number of modes depends on the cross-section type and the number of fold lines [23]. GBT has been applied to composite beams in [24]. Higher-order theories [25–37] are obtained using refined displacement models for the cross-section displacement field. Washizu [38] clearly stated how the use of arbitrary rich displacement fields can lead to exact 3D solutions; the main issue of using arbitrary rich models is represented by the difficulty of dealing with an increasing number of equations. An important effort to apply refined beam models to aeroelastic problems was made by Librescu and his co-workers who incorporated a number of non-classical effects in order to study the static and dynamic aeroelastic response of composite beam structures [39]. When 'soft-in-shear' composite materials are considered, e.g. sandwich structures having soft cores, a proper structural analysis often requires the exploitation of Layer-Wise models and mixed formulations which consider shear stresses as primary variables of the problem. Comprehensive and detailed analyses about these issues can be found in Carrera and Ciuffreda [40] and in Carrera and Brischetto [41,42].

This paper is a companion work of [43], where flutter analyses of isotropic structures were considered. The Carrera Unified Formulation (CUF) for higher-order 1D models [44] was exploited to develop structural theories. CUF has been initially developed for plates and shells [45,46], and more recently for beams [47,48]. The unique contribution given by CUF models is due to their hierarchical capabilities which make the choice of the expansion functions (F_τ) and their order arbitrary. This means that any-order structural models can be implemented with no need of formal changes in the problem equations and matrices. CUF can therefore deal with arbitrary geometries, boundary conditions and material characteristics with no need of *ad hoc* formulations.

Static [48–50], free-vibration [51–53] and buckling [54,55] analyses showed the enhanced capabilities of CUF 1D models which are able to detect shell- and solid-like solutions for different structural models including thin-walled models under point loads and shell-like natural modes. A further extension of the present formulation [56–58] dealt with open cross-sections, boundary conditions enforced on lateral edges and component-wise approaches.

This paper is organized as follows: first, CUF and the aeroelastic formulation based on DLM are briefly described; afterwards, results and their discussion are presented in terms of natural modes and flutter conditions; eventually main conclusions are drawn.

2. Structural formulation: CUF 1D models

The structural formulation exploited for the aeroelastic analysis is described in this section. The Carrera Unified Formulation is first described. Afterwards, the finite element formulation and the extension to composites are dealt with.

2.1. One-dimensional structural models with variable kinematics

The unified formulation of the beam cross-section displacement field is described by an expansion of generic functions, F_τ,

$$\mathbf{u} = F_\tau \mathbf{u}_\tau, \quad \tau = 1, 2, \ldots, M \tag{1}$$

where F_τ are functions of the cross-section coordinates x and z, $\mathbf{u}_\tau$ is the displacement vector, and M stands for the number of terms of the expansion. According to the Einstein notation, the repeated subscript τ indicates summation. The choice of F_τ and M is arbitrary, that is, different base functions of any-order can be taken into account to model the displacement field of a beam above its cross-section. In this work, Taylor-like polynomial expansions ($x^i z^j$) of the displacement field above the cross-section of the structure were used, where i and j are positive integers. The order N of the expansion is arbitrary and is set as an input of the analysis. The choice of N for a given structural problem is usually made through a convergence study. For example, the second-order model, $N = 2$, is based on the following displacement field:

$$\begin{aligned} x &= u_{x_1} + x\,u_{x_2} + z\,u_{x_3} + x^2\,u_{x_4} + xz\,u_{x_5} + z^2\,u_{x_6} \\ y &= u_{y_1} + x\,u_{y_2} + z\,u_{y_3} + x^2\,u_{y_4} + xz\,u_{y_5} + z^2\,u_{y_6} \\ z &= u_{z_1} + x\,u_{z_2} + z\,u_{z_3} + x^2\,u_{z_4} + xz\,u_{z_5} + z^2\,u_{z_6} \end{aligned} \tag{2}$$

The 1D model described by Eq. (2) has 18 generalized displacement variables: three constant, six linear, and nine parabolic terms. It is important to underline that in the CUF framework

1. The order N is arbitrary. This means that N can be opportunely increased to obtain the desired level of accuracy,
2. The choice of the expansion functions F_τ is arbitrary too. For instance, Lagrange polynomials or harmonics can be used to define the cross-section displacement field.

2.2. Finite element formulation and extension to composites

The governing equations were derived by means of the Principle of Virtual Displacements (PVDs). Starting from the unified form of the displacement field in Eq. (1), stiffness, mass, and loading arrays can be obtained in terms of fundamental nuclei whose form is independent of the order of the model. The finite element method (FEM) was adopted to overcome the limitations of analytical solutions in terms of geometry, loading, and boundary conditions. The displacement variables are interpolated along the axis of the beam by means of the shape functions, N_i

$$\mathbf{u} = N_i F_\tau \mathbf{q}_{\tau i} \tag{3}$$

where $\mathbf{q}_{\tau i}$ is the nodal displacement vector. Beam elements with four - here denoted as B4 - nodes were considered in this paper. It is important to underline that the beam model order is given by the expansion on the cross-section whereas the number of nodes per each element is related to the approximation along the

longitudinal axis of the beam (y). An N-order beam model is therefore a theory that exploits an N-order Taylor-like polynomial to describe the kinematics of the beam cross-section.

According to the principle of virtual displacements

$$\delta L_{int} = \int_V (\delta[\epsilon]^T[\sigma])dV = \delta L_{ext} \tag{4}$$

where L_{int} stands for the strain energy, L_{ext} is the work of the external loadings, δ stands for the virtual variation, $[\sigma]$ is the stress vector and $[\epsilon]$ is the strain vector. A compact form of the virtual variation of the strain energy can be obtained as shown in [44]

$$\delta L_{int} = \delta \mathbf{q}_{\tau i}^T \mathbf{K}^{ij\tau s} \mathbf{q}_{sj} \tag{5}$$

where $\mathbf{K}^{ij\tau s}$ is the stiffness matrix written in the form of the fundamental nuclei. Superscripts indicate the four indexes exploited to assemble the matrix: i and j are related to the shape functions, τ and s are related to the expansion functions. The fundamental nucleus is a 3×3 array which is formally independent of the order of the beam model. In a compact notation, the stiffness matrix for a given material property set can be written as:

$$\begin{aligned}
\mathbf{K}^{ij\tau s} = {} & I_l^{ij} \triangleleft \left(\mathbf{D}_{np}^T F_\tau \mathbf{I}\right)\left[\widetilde{\mathbf{C}}_{np}(\mathbf{D}_p\ F_s\ \mathbf{I}) + \widetilde{\mathbf{C}}_{nn}\ (\mathbf{D}_{np}\ F_s\ \mathbf{I})\right] \\
& + \left(\mathbf{D}_p^T\ F_\tau\ \mathbf{I}\right)\left[\widetilde{\mathbf{C}}_{pp}\ (\mathbf{D}_p\ F_s\ \mathbf{I}) + \widetilde{\mathbf{C}}_{pn}\ (\mathbf{D}_{np}\ F_s\ \mathbf{I})\right] \triangleright_\Omega + I_l^{ij,y} \\
& \triangleleft \left[(\mathbf{D}_{np}^T\ F_\tau\ \mathbf{I})\ \widetilde{\mathbf{C}}_{nn} + \left(\mathbf{D}_p^T\ F_\tau\ \mathbf{I}\right)\ \widetilde{\mathbf{C}}_{pn}\right] F_s \triangleright_\Omega \mathbf{I}_{\Omega y} + I_l^{i,yj}\ \mathbf{I}_{\Omega y} \\
& \triangleleft F_\tau\ \left[\widetilde{\mathbf{C}}_{np}\ (\mathbf{D}_p\ F_s\ \mathbf{I}) + \widetilde{\mathbf{C}}_{nn}\ (\mathbf{D}_{np}\ F_s\ \mathbf{I})\right] \triangleright_\Omega + I_l^{i,yj,y}\ \mathbf{I}_{\Omega y} \\
& \triangleleft F_\tau \widetilde{\mathbf{C}}_{nn} F_s \triangleright_\Omega \mathbf{I}_{\Omega y}
\end{aligned} \tag{6}$$

where

$$\mathbf{I} = \begin{bmatrix} 1 & 0 & 0 \\ 0 & 1 & 0 \\ 0 & 0 & 1 \end{bmatrix} \mathbf{I}_{\Omega y} = \begin{bmatrix} 0 & 1 & 0 \\ 1 & 0 & 0 \\ 0 & 0 & 1 \end{bmatrix} \triangleleft \cdots \triangleright_\Omega = \int_\Omega \cdots d\Omega \tag{7}$$

$$\left(I_l^{ij},\ I_l^{ij,y},\ I_l^{i,yj},\ I_l^{i,yj,y}\right) = \int_l \left(N_i\ N_j,\ N_i\ N_{j,y},\ N_{i,y}\ N_j,\ N_{i,y}\ N_{j,y}\right) dy \tag{8}$$

$\widetilde{\mathbf{C}}$ is the material coefficient matrix and $\mathbf{D}$ is the differential operator matrix. For the sake of brevity, their expressions are not reported here, they can be found in [44]. It should be underlined that the formal expression of $\mathbf{K}^{ij\tau s}$

1. does not depend on the expansion order,
2. does not depend on the choice of the F_τ expansion polynomials.

These are the key-point of CUF which permits, with only nine FORTRAN statements, to implement any-order of multiple class theories.

The virtual variation of the work of the inertial loadings is

$$\delta L_{ine} = \int_V \rho[\ddot{\mathbf{u}}]\delta[\mathbf{u}]^T dV \tag{9}$$

where ρ stands for the density of the material, and $[\ddot{\mathbf{u}}]$ is the acceleration vector. Eq. (9) can be rewritten in a compact manner as follows:

$$\delta L_{ine} = \delta \mathbf{q}_{\tau i}^T \mathbf{M}^{ij\tau s} \ddot{\mathbf{q}}_{sj} \tag{10}$$

where $\mathbf{M}^{ij\tau s}$ is the mass matrix in the form of the fundamental nucleus whose components can be found in [57].

The undamped dynamic problem can be written as follows:

$$\mathbf{M}\ddot{\mathbf{a}} + \mathbf{K}\mathbf{a} = \mathbf{p} \tag{11}$$

where $[\mathbf{a}]$ is the vector of the nodal unknowns and $\mathbf{p}$ is the loading vector. Introducing harmonic solutions, it is possible to compute the natural frequencies, Ω_i, for the homogenous case, by solving an eigenvalue problem

$$(-\Omega_i^2 \mathbf{M} + \mathbf{K})[\phi]_i = 0 \tag{12}$$

where $[\phi]_i$ is the ith eigenvector.

A CUF 1D model can deal with nonhomogeneous composite structures by two modeling approaches

1. The equivalent single-layer approach (ESL).
2. The layerwise approach (LW).

In an ESL model, the homogenization of the properties of each layer is conducted by summing the contributions of each layer in the stiffness and mass matrices. This process leads to a model that has a set of variables that is assumed for the whole multilayer. On the other hand, LW considers different sets of variables per each layer, and the homogenization is just conducted at the interface level. In this paper, ESL was considered since it offers good accuracy for the structural configurations and mechanical problems herein addressed, as also shown in [57].

3. Aeroelastic formulation

The aeroelastic formulation is described in this section. First, the doublet lattice method is briefly introduced together with the splining method adopted. Then the aerodynamic and structural generalized meshes are given and the g-method briefly described.

3.1. Doublet lattice method and mesh-to-mesh transformations

Following Landahl [59] or Albano [3], the normalwash in a point with coordinates x, y due to the pulsating pressure jump $\overline{\Delta p}$ in the point $\xi,\ \eta$ has the following expression:

$$\overline{w} = \frac{1}{8\pi} \int_A \overline{\Delta p} K(x_0, y_0, \omega, M) dA \tag{13}$$

where M is the Mach number and ω is the circular frequency and

$$x_0 = x - \xi; \quad y_0 = y - \eta \tag{14}$$

The kernel function (K) formal expression is not reported here for the sake of brevity, it can be found in [59]. Eq. (13) can be numerically solved by means of the doublet lattice method (DLM). In the DLM framework a lifting surface is discretized in a number of panels and the following algebraic system of equations has to be solved:

$$\overline{w}_i = \sum_{j=1}^{N_P} D_{ij} \overline{\Delta p}_j \tag{15}$$

where N_P indicates the total number of aerodynamic panels and D_{ij} is the normalwash factor. In this paper D_{ij} was calculated by exploiting Rodden's quartic DLM [4]. For the sake of brevity, the procedure to compute the normalwash factor is not reported here, it can be found in Rodden's paper. It is important to underline that the steady contribution to D_{ij} was computed via the vortex lattice method (VLM) [60].

The unsteady aeroelastic analysis was carried out by considering a set of modal shapes as generalized motions for the unsteady aerodynamic generalized force generation. Each set of modal shapes, $[\phi]_m$, was defined on a set of points above the structure. Slopes and displacements at control and load points of the aerodynamic panels are then given by

$$\frac{\partial \mathcal{Z}_m}{\partial x} = \boldsymbol{A} \cdot \boldsymbol{\phi}_m \tag{16}$$

$$\widetilde{\mathcal{Z}}_m == \widetilde{\boldsymbol{A}}^{\star} \cdot \boldsymbol{\phi}_{\mathbf{m}} \tag{17}$$

$$\mathcal{Z}_{\mathrm{m}} == \boldsymbol{A}^{\star} \cdot \boldsymbol{\phi_m} \tag{18}$$

where $\boldsymbol{A}, \widetilde{\boldsymbol{A}}^{\star}$ and $\boldsymbol{A}^{\star}$ were computed through the Infinite Plate Spline (IPS) [61]. For the sake of brevity, the explicit expressions of these matrices are not reported here, they can be found in [62]. IPS was chosen in order to better exploit the shell-like capabilities of the present 1D structural formulation, as shown by Varello et al. [63]. Under the assumption of simple harmonic motion, it is possible to demonstrate that the vector that contains the normalized (using the velocity V_∞ parallel to x) normalwash has the following expression (the boundary condition is enforced on all control points of the lifting surface):

$$\boldsymbol{w}_m = i\frac{\omega}{V_\infty}\mathcal{Z}_{\mathrm{m}} + \frac{\partial \mathcal{Z}_{\mathrm{m}}}{\partial x} \tag{19}$$

where i is the imaginary unit and all the vector quantities have to be understood as vectors of amplitudes of the harmonic motion.

3.2. Generalized matrices and g-method

The generalized aerodynamic matrix for a given reduced frequency (k) is given by

$$Q_{ij}(ik) = \sum_{N=1}^{N_{AP}} \Delta p_j^N(ik)\ \widetilde{\mathcal{Z}}_{\mathrm{i}}^N\ A^N \tag{20}$$

where

- $k = \omega b/L$, b is the reference length (equal to the half of the reference chord) and L is the length of the structure.
- $\Delta p_j^N(ik)$ is the pressure jump due to the jth set of motions (modal shapes), acting on the Nth aerodynamic panel and evaluated for a given reduced frequency. The computation of the pressure jump is performed by means of the DLM.
- $\widetilde{\mathcal{Z}}_{\mathrm{i}}^N$ is the ith motion set evaluated at the Nth aerodynamic panel. Starting from the ith modal shape given by a structural model, the ith motion set is then mapped on the aerodynamic panels by means of the splining process. In this work, modal shapes were evaluated by means of CUF 1D models.
- A^N is the area of the Nth panel.

$\mathbf{Q}(ik)$ is a square matrix with $N_{modes} \times N_{modes}$ elements, where N_{modes} indicates the total number of natural modes adopted. Typically, N_{modes} ranges from 10 to 20.

The generalized mass matrix is given by

$$\widetilde{\mathbf{M}} = [\phi]^T\ \mathbf{M}\ [\phi] \tag{21}$$

where $[\phi]$ is a matrix containing a given number of modal shapes. The generalized stiffness matrix is a square diagonal matrix, its terms are given by

$$\widetilde{K}_{ii} = \omega_i^2\ \widetilde{M}_{ii} \tag{22}$$

where ω_i is the oscillatory frequency associated to the ith modal shape.

The g-method was introduced by Chen [64] and it is based on a damping perturbation technique and a first order model of the damping term. Its derivation exploits the aerodynamics in the Laplace domain and can be found in [64]. The basic assumption of the g-method is based on the following approximation of the generalized aerodynamic matrix:

$$\widetilde{\mathbf{Q}}(p) \approx \widetilde{\mathbf{Q}}(ik) + g\widetilde{\mathbf{Q}}'(ik), \quad for \quad g \ll 1 \tag{23}$$

where $g = \gamma k$ and γ is the transient decay rate coefficient. Eq. (23) leads to the g-method equation:

$$\left[\left(\frac{V_\infty}{b}\right)^2 \widetilde{\mathbf{M}}\, p^2 + \tilde{\mathbf{K}} - \frac{1}{2}\rho V_\infty^2\, \widetilde{\mathbf{Q}}'(ik)\, g - \frac{1}{2}\rho V_\infty^2\, \widetilde{\mathbf{Q}}(ik)\right]\{\mathbf{q}(p)\} = \mathbf{0} \tag{24}$$

where p is the nondimensional Laplace parameter ($p = g + ik$) and b is the reference length (usually equal to the half of the reference chord).

The generalized aerodynamic matrix, $\widetilde{\mathbf{Q}}(ik)$, is provided by the unsteady aerodynamic model (DLM) in the frequency domain. $\widetilde{\mathbf{Q}}(ik)$ is then obtained for a given number of k values and the computation of $\widetilde{\mathbf{Q}}'(ik)$ has to be performed numerically. A central difference scheme can be used and a forward one at $k = 0$. Three new matrices are introduced,

$$\begin{aligned}
\mathbf{A} &= \left(\frac{V_\infty}{b}\right)^2 \widetilde{\mathbf{M}} \\
\mathbf{B} &= 2ik\left(\frac{V_\infty}{b}\right)^2 \widetilde{\mathbf{M}} - \frac{1}{2}\rho V_\infty^2\, \widetilde{\mathbf{Q}}'(ik) \\
\mathbf{C} &= -k^2\left(\frac{V_\infty}{b}\right)^2 \widetilde{\mathbf{M}} + \tilde{\mathbf{K}} - \frac{1}{2}\rho V_\infty^2\, \widetilde{\mathbf{Q}}(ik)
\end{aligned} \tag{25}$$

Eq. (24) becomes

$$\left[g^2\mathbf{A} + g\mathbf{B} + \mathbf{C}\right]\{\mathbf{q}\} = 0 \tag{26}$$

This is a second-order linear system in g, the g-method targets to find those solutions having Im (g) = 0. Eq. (26) is rewritten in the state-space form

$$[\mathbf{D} - g\mathbf{I}]\{\mathbf{X}\} = 0 \tag{27}$$

where

$$\mathbf{D} = \begin{bmatrix} \mathbf{0} & \mathbf{I} \\ -\mathbf{A}^{-1}\mathbf{C} & -\mathbf{A}^{-1}\mathbf{B} \end{bmatrix} \tag{28}$$

A so-called *reduced-frequency-sweep technique* is adopted to find the solution having Im (g) = 0. For the sake of brevity, the detailed description of this technique is not reported here, it can be found in [64].

4. Results and Discussion

Flutter analyses of composite wings were carried out on models retrieved from [65,66]. A graphite/epoxy composite material was used, E_L = 98.0 GPa, E_T = 7.90 GPa, G_{LT} = 5.60 GPa, ν = 0.28 and ρ = 1520 kg/m^3. Fig. 1 shows the fiber orientation angle, θ and the sweep angle, Λ. The length of the wing, L, is equal to 305 mm; the chord, c, is equal to 76.2 mm. All the results were obtained in the case of incompressible flow ($M = 0$).

4.1. 1D model expansion order and mesh effect studies

The effect of the 1D model order (N) and the effect of the structural and aerodynamic meshes were investigated in this section. A straight wing ($\Lambda = 0$) having a symmetric six-layer lamination was considered, the stacking sequence being $[30_2/0]_s$; the total

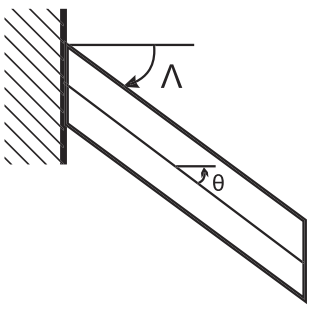

Fig. 1. Sweep and fiber orientation angles.

Table 1
Effect of the CUF 1D expansion order, N, on the first natural frequencies (Hz) of the $[30_2/0]_s$ straight wing, 15 B4 mesh.

Model	f_1	f_2	f_3	f_4	f_5	DOFs
EBBT	7.407	46.421	129.978	254.701	421.032	138
TBT	7.389	46.306	129.644	254.009	419.809	230
$N = 1$	7.389	46.303	129.633	253.984	419.756	414
$N = 2$	6.111	36.594	69.170[a]	103.860	208.469	828
$N = 3$	6.073	36.174	57.310[a]	100.956	177.263[a]	1380
$N = 4$	6.059	35.918	56.510[a]	100.034	172.233[a]	2070

[a] Torsional mode.

Table 2
Effect of the expansion order on flutter conditions of the $[30_2/0]_s$ wing, 15 B4 mesh.

Model	Velocity (m/s)	Frequency (Hz)	DOFs
$N = 2$	28.820	27.813	828
$N = 3$	25.938	26.651	1380
$N = 4$	25.864	26.666	2070

Table 3
Effect of the structural mesh on flutter conditions of the $[30_2/0]_s$ straight wing, $N = 3$.

Mesh	Velocity (m/s)	Frequency (Hz)
10 B4	25.939	26.651
15 B4	25.938	26.651
20 B4	25.937	26.650

Table 4
Effect of the aerodynamic mesh on flutter conditions of the $[30_2/0]_s$ straight wing, $N = 4$, 15 B4 mesh.

Mesh	Velocity (m/s)	Frequency (Hz)
8×20	25.736	26.923
8×30	25.864	26.666
8×40	25.932	26.526

thickness of the laminate is 0.804 mm with constant thickness layers.

Table 1 shows the first five natural frequencies of the structure for different models. Unless otherwise indicated, the frequencies reported in this table are related to bending modes. The total number of degrees of freedom (DOFs) of each model is given in the last column of the table. Table 2 presents the effect of N on flutter velocities and frequencies. Second-, third- and fourth-order models were considered. Lower-order models (EBBT, TBT and $N = 1$), in fact, are not able to detect correct flutter conditions for this kind of structure. Mesh effects on flutter conditions are shown in Tables 3 and 4. Fig. 2 shows the damping and the frequency of the first two natural modes vs. the free-stream velocity. It can be observed that flutter occurs with the coalescence of these modes. The results obtained suggest the following:

1. Lower-order structural models (EBBT, TBT and $N = 1$) can detect bending modes. However bending frequencies from these models are poorly accurate. This is most likely due to the combined effect of the material inhomogeneity and of the thin cross-section. On the other hand, torsional modes cannot be detected by these models.
2. An $N = 2$ model is able to compute bending frequencies with satisfactory accuracies and to detect torsional frequencies. At least an $N = 3$ model is necessary to detect accurate torsional frequencies.
3. The proper expansion order for the flutter analysis is strictly related to the model required by the free vibration analysis. At least an $N = 3$ model is required for flutter, the $N = 2$ model, in fact, slightly overestimates flutter velocity and frequency. The $N = 2$ model error can be even larger when torsional modes are involved in flutter, as shown in [43].
4. The influence of the aerodynamic and structural mesh is far less important than the Taylor expansion order to compute flutter conditions.
5. The computational costs of the present 1D CUF models are low compared to typical plate or solid models.

4.2. Straight wing and stacking sequence effect

In this section, different symmetric stacking sequences were considered. The same straight wing considered in the previous section was first analyzed. Table 5 shows flutter conditions for four different stacking sequences. Results from the present $N = 4$ 1D models were compared with those from a plate (Classical Laminate Theory, CLT) and with experimental data. Table 6 shows vibration frequencies (bending and torsional) and flutter conditions for a symmetric eight layer structure. The total thickness of the laminate is equal to 1.072 mm. The stacking sequence is $[-22.5/67.5/22.5/-67.5]_s$. The thickness sequence is $[0.09/0.12/0.16/0.63]_s$, where each term indicates the thickness ratio of each ply with respect to the half of the thickness of the laminate. For instance, the thickness of the first layer is the 9% of the half thickness of the laminate. Results were compared to those from a CLT model. Results suggest the following:

1. An excellent match was found between the results from the present 1D structural formulation and CLT models. Both torsional modes and flutter conditions were, in fact, computed by the $N = 4$ with very low differences with respect to the 2D structural model.
2. Slightly poorer match was found with the experimental results.
3. As it was expected, changes in the stacking sequences can lead to very different flutter conditions.

4.3. Swept wing

A backward swept wing was considered as the last assessment of this paper. The sweep angle (Λ) equal to 30°. The total thickness of the laminate equal to 1.072 mm. The stacking sequence is $[-22.5/67.5/22.5/-67.5]_s$, The thickness sequence is $[0.09/0.12/0.16/0.63]_s$.

Natural frequencies were first computed, those related to the first five modes (bending and torsional) are shown in Table 7. Results from 2D structural models are also reported. Flutter conditions computed via different CUF models, structural and aerodynamic meshes are reported in Tables 8–10, respectively. The results obtained suggest the following:

1. The combined effect of the material inhomogeneity, thin cross-section and sweep angle makes the use of refined 1D structural models even more necessary than the previous straight configurations. The sweep angle makes, in fact, the accuracy of lower-order models poorer than in the case of the straight wing.
2. The accuracy of the $N = 2$ model for flutter is poorer than in the straight wing case. The proper modeling of the bending/torsion coupling due to the sweep angle requires, in fact, at least an $N = 3$ model.

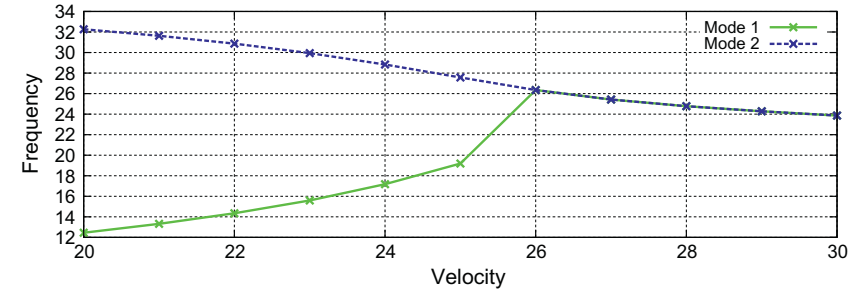

(a) Frequency

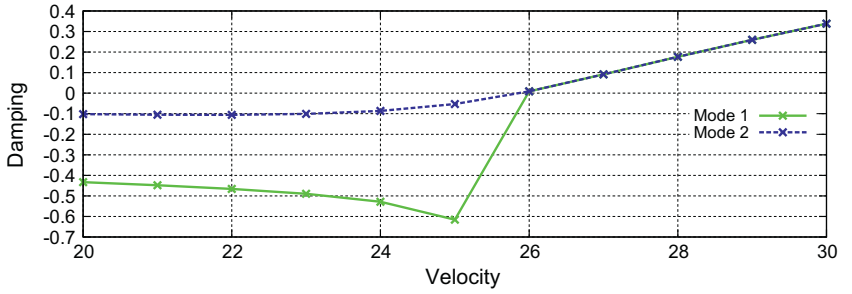

(b) Damping

Fig. 2. Frequency and damping of mode 1 and 2 vs. velocity of the $[30_2/0]_s$ straight wing, 15 B4 mesh, $N = 4$.

Table 5
Flutter velocities [m/s] for a six layer laminated straight wing, $N = 4$, 15 B4 mesh, 8×30 panels.

Lamination	$N = 4$	[65] (CLT)	[66] (Exp)
$[0_2/90]_s$	23.2	23.0	25
$[+45/-45/0]_s$	40.3	40.1	> 32
$[45_2/0]_s$	26.2	27.5	28
$[30_2/0]_s$	25.9	27.1	27

Table 6
Vibration frequencies [Hz] and flutter velocities [m/s] for an eight-layer straight wing, $N = 4$, 15 B4 mesh, 8×30 panels.

Model	f_1	f_2	f_3	f_4	f_5	V_F
$N = 4$	7.2	45.1	58.9[b]	126.5	181.9[b]	38.2
[65] (CLT)	7.3	45.4	59.1[b]	127.7	182.3[b]	38.8

[b] Torsional mode.

Table 7
Effect of the CUF 1D expansion order, N, on vibration frequencies of the eight-layer swept wing, 15 B4 mesh.

Model	f_1	f_2	f_3	f_4	f_5	DOFs
EBBT	6.7	42.2	118.3	231.8	383.1	138
TBT	6.7	42.2	118.3	231.7	382.9	230
$N = 1$	6.7	42.2	118.2	231.7	382.9	414
$N = 2$	5.6	34.8	75.7[c]	97.6	193.5	828
$N = 3$	5.6	34.4	59.6[c]	95.9	182.7[c]	1380
$N = 4$	5.6	34.2	58.9[c]	95.4	178.1[c]	2070
[65] (CLT)	5.6	34.4	60.0[c]	95.4	182.0[c]	–

[c] Torsional mode.

Table 8
Effect of the expansion order on flutter conditions of the eight-layer swept wing, 15 B4 mesh.

Model	Velocity (m/s)	Frequency (Hz)	DOFs
$V_{ref} = 32.4$ [65]			
$N = 2$	38.703	28.394	828
$N = 3$	31.957	26.479	1380
$N = 4$	31.688	26.523	2070

Table 9
Effect of the structural mesh on flutter conditions of the eight-layer swept wing, $N = 3$.

Mesh	Velocity (m/s)	Frequency (Hz)
10 B4	31.911	26.400
15 B4	31.957	26.479
20 B4	31.996	26.445

Table 10
Effect of the aerodynamic mesh on flutter conditions of the eight-layer swept wing, $N = 4$, 15 B4 mesh.

Mesh	Velocity (m/s)	Frequency (Hz)
8×20	31.577	26.733
8×30	31.688	26.523
8×40	31.744	26.414

3. Results from the present 1D CUF structural model are in excellent agreement with those from literature. It can be stated that plate-like accuracies can be obtained by adopting an $N = 3$ or an $N = 4$ CUF 1D model. Low computational costs are required.

4. As for the straight wing case, the structural and aerodynamic meshes adopted barely affect the accuracy of the results.

5. Conclusion

Flutter analyses of composite lifting surfaces have been presented in this paper. 1D refined structural models and the doublet lattice method have been employed to develop an advanced aeroelastic formulation. The aerodynamic and structural mesh coupling has been conducted through the infinite plate spline method. Flutter conditions have been computed via the g-method.

The Carrera Unified Formulation (CUF) has been used to build the structural component of the aeroelastic formulation. In this pa-

per, CUF 1D models exploit Taylor-like polynomials to define the displacement field above the cross-section of the beam. Any-order structural models can be implemented since the order of the Taylor expansion is a free-parameter of the formulation. This means that the order of the structural model can be set as an input and convergence studies have to be carried out in order to establish the proper theory order necessary for a given problem.

The analyses conducted suggest the following:

1. Classical (EBBT and TBT) and lower-order ($N = 1$ and $N = 2$) are inadequate for the flutter analysis of typical lifting surfaces made of composite materials.
2. Refined 1D structural models are mandatory for proper flutter analyses of lifting surfaces. In particular, at least a third-order model ($N = 3$) should be employed.
3. Refinements are needed to capture torsional modal shapes and to deal with thin walls, inhomogeneity and bending/torsion coupling.
4. The present 1D structural model is cost-competitive if compared to 2D plate models with no accuracy losses.

The use of CUF 1D could offer even greater advantages in the fluid–structure-interaction analysis of flexible structures with highly deformable cross-section, such as adaptive wings or arteries. CUF 1D can, in fact, predict in-plane distortion of thin-walled structure with high accuracy and very low computational costs, as shown in [44]. Future works should deal with the coupling of CUF 1D with computational fluid dynamics tools and the extensions to structural non-linearities.

Acknowledgements

The financial supports of the Italian Fulbright Commission and of the European Project SARISTU are gratefully acknowledged. The author warmly thanks Prof. Luciano Demasi (San Diego State University) and Prof. Erasmo Carrera (Politecnico di Torino) for their helpful efforts in helping him in the research activity related to this paper.

References

[1] Yurkovich R. Status of unsteady aerodynamic prediction for flutter of high-performance aircraft. J Aircr 2003;40(5):832–42.
[2] Schuster DM, Liu DD, Huttsell LJ. Computational aeroelasticity: success, progress challenge. J Aircr 2003;40(5):843–56.
[3] Albano E, Rodden WP. A doublet-lattice method for calculating lift distributions on oscillating surfaces in subsonic flows. AIAA J 1969;7(2):279–85.
[4] Rodden WP, Taylor PF, McIntosh Jr SC. Further refinement of the subsonic doublet-lattice method. J Aircr 1998;35(5):720–6.
[5] Bernoulli D. Commentarii academiae scientiarum imperialis petropolitanae, chapter De vibrationibus et sono laminarum elasticarum. Petropoli; 1751.
[6] Euler L. De curvis elasticis. Bousquet: Lausanne and Geneva; 1744.
[7] Timoshenko SP. On the corrections for shear of the differential equation for transverse vibrations of prismatic bars. Philos Mag 1921;41:744–6.
[8] Tsai SW. Composites design. Think composites, 4th ed., Dayton: 1988.
[9] Kapania K, Raciti S. Recent advances in analysis of laminated beams and plates, Part I: Shear effects and buckling. AIAA J 1989;27(7):923–35.
[10] Reddy JN. On locking-free shear deformable beam finite elements. Comput Methods Appl Mech Eng 1997;149:113–32.
[11] Timoshenko SP, Goodier JN. Theory of elasticity. New York: McGraw-Hill; 1970.
[12] Sokolnikoff IS. Mathematical theory of elasticity. McGrw-Hill; 1956.
[13] Gruttmann F, Sauer R, Wagner W. Shear stresses in prismatic beams with arbitrary cross-sections. Int J Numer Methods Eng 1999;45:865–89.
[14] Goyal VK, Kapania RK. A shear-deformable beam element for the analysis of laminated composites. Finite Elem Anal Des 2007;43:463–77.
[15] El Fatmi R, Ghazouani N. Higher order composite beam theory built on Saint-Venantś solution, Part-I: Theoretical developments. Compos Struct 2011;93(2). http://dx.doi.org/10.1016/j.compstruct.2010.08.024.
[16] Barradas Cardoso JE, Benedito NMB, Anibal JJV. Finite element analysis of thin-walled composite laminated beams with geometrically nonlinear behavior including warping deformation. Thin-Walled Struct 2009;47:1363–72. http://dx.doi.org/10.1016/j.tws.2009.03.002.
[17] Ladéveze P, Simmonds J. New concepts for linear beam theory with arbitrary geometry and loading. Euro J Mech – A/Solids 1998;17(3):377–402.
[18] Berdichevsky VL, Armanios E, Badir A. Theory of anisotropic thin-walled closed-cross-section beams. Compos Eng 1992;2(5–7):411–32.
[19] Cesnik CES, Sutyrin VG, Hodges DH. Refined theory of composite beams: the role of short-wavelength extrapolation. Int J Solid Struct 1996;33(10):1387–408.
[20] Volovoi VV, Hodges DH. Theory of anisotropic thin-walled beams. J Appl Mech 2000;67(3):453–9.
[21] Yu W, Volovoi VV, Hodges DH, Hong X. Validation of the variational asymptotic beam sectional analysis (VABS). AIAA J 2002;40(10):2105–13.
[22] Schardt R. Eine erweiterung der technischen biegetheorie zur berechnung prismatischer faltwerke. Der Stahlbau 1966;35:161–71.
[23] Nedelcu M. GBT formulation to analyse the behaviour of thin-walled members with variable cross-section. Thin-Walled Struct 2010;48(8):629–38.
[24] Silvestre N, Camotim D. First-order generalised beam theory for arbitrary orthotropic materials. Thin-Walled Struct 2002;40(9):791–820.
[25] Averill RC, Yuen CY. Development of simple robust finite elements based on refined theories for thick laminated beams. Comput Struct 1996;59(3):529–46. http://dx.doi.org/10.1016/0045-7949(95)00269-3.
[26] Taufik A, Barrau JJ, Lorin F. Composite beam analysis with arbitrary cross section. Compos Struct 1999;44:189–94. http://dx.doi.org/10.1016/S0263-8223(98)00134-2.
[27] Song SJ, Waas AM. Effects of shear deformation on buckling and free vibration of laminated composite beams. Compos Struct 1997;37(1):33–43.
[28] Maddur SS, Chaturvedi SK. Laminated composite open profile sections: non-uniform torsion of I-sections. Compos Struct 2000;50:159–69. http://dx.doi.org/10.1016/S0263-8223(00)00093-3.
[29] Khdeir AA, Reddy JN. An exact solution for the bending of thin and thick cross-ply laminated beams. Compos Struct 1997;37:195–203. http://dx.doi.org/10.1016/S0263-8223(97)80012-8.
[30] Shi G, Lam KY, Tay TE. On efficient finite element modeling of composite beams and plates using higher-order theories and an accurate composite beam element. Compos Struct 1998;41:159–65. http://dx.doi.org/10.1016/S0263-8223(98)00050-6.
[31] Sapountzakis EJ, Mokos VG. 3-D beam element of composite cross section including warping and shear deformation effects. Comput Struct 2007;85:102–16. http://dx.doi.org/10.1016/j.compstruc.2006.09.003.
[32] Chen W, Wu Z. A new higher-order shear deformation theory and refined beam element of composite laminates. Acta Mech Sinica 2005;21:65–9. http://dx.doi.org/10.1007/s10409-005-0011-4.
[33] Kim C, White SR. Thick-walled composite beam theory including 3-D elastic effects and torsional warping. Int J Solid Struct 1997;34(31–32):4237–59. http://dx.doi.org/10.1016/S0020-7683(96)00072-8.
[34] Bathe SR, Nayak UN, Patki AV. Deformation of composite beam using refined theory. Comput Struct 1995;54(3):541–6. http://dx.doi.org/10.1016/0045-7949(94)00354-6.
[35] Rand O. On the importance of cross-sectional warping in solid composite beams. Compos Struct 2000;49:393–7. http://dx.doi.org/10.1016/S0263-8223(00)00073-8.
[36] Lee J. Flexural analysis of thin-walled composite beams using shear-deformable beam theory. Compos Struct 2005;70(2):212–22. http://dx.doi.org/10.1016/j.compstruct.2004.08.023.
[37] Soldatos KP, Watson P. A general theory for the accurate stress analysis of homogenous and laminated composite beams. Int J Solids Struct 1997;34(22):2857–85. http://dx.doi.org/10.1016/S0020-7683(96)00170-9.
[38] Washizu K. Variational methods in elasticity and plasticity. Oxford: Pergamon Press; 1968.
[39] Librescu L, Song O. On the static aeroelastic tailoring of composite aircraft swept wings modelled as thin-walled beam structures. Compos Eng 1992;2:497–512.
[40] Carrera E, Ciuffreda A. Bending of composites and sandwich plates subjected to localized lateral loadings: a comparison of various theories. Compos Struct 2005;68(2):185–202.
[41] Carrera E, Brischetto S. A survey with numerical assessment of classical and refined theories for the analysis of sandwich plates. Appl Mech Rev 2009;62(1).
[42] Carrera E, Brischetto S. A comparison of various kinematic models for sandwich shell panels with soft core. J Compos Mater 2009;43(20):2201–21.
[43] Petrolo M. Advanced 1d structural models for flutter analysis of lifting surfaces. Int. J of Aeronautical & Space Sci 2012;13(2):199–209. http://dx.doi.org/10.5139/IJASS.2012.13.2.199.
[44] Carrera E, Giunta G, Petrolo M. Beam structures: classical and advanced theories. John Wiley & Sons; 2011.
[45] Carrera E. Theories and finite elements for multilayered anisotropic composite plates and shells. Arch Comput Methods Eng 2002;9(2):87–140.
[46] Carrera E. Theories and finite elements for multilayered plates and shells: a unified compact formulation with numerical assessment and benchmarking. Arch Comput Methods Eng 2003;10(3):216–96.
[47] Carrera E, Giunta G. Refined beam theories based on a unified formulation. Int J Appl Mech 2010;2(1):117–43.
[48] Carrera E, Giunta G, Nali P, Petrolo M. Refined beam elements with arbitrary cross-section geometries. Comput Struct 2010;88(5–6):283–93. http://dx.doi.org/10.1016/j.compstruc.2009.11.002.
[49] E. Carrera, G. Giunta, M. Petrolo, A modern and compact way to formulate classical and advanced beam theories, Stirlingshire (UK): Saxe-Coburg Publications; 2010. p. 75–112. doi:10.4203/csets.25.4 [chapter 4].

[50] Carrera E, Petrolo M, Zappino E. Performance of cuf approach to analyze the structural behavior of slender bodies. J Struct Eng 2012;138(2). http://dx.doi.org/10.1061/(ASCE)ST.1943-541X.0000402.
[51] Carrera E, Petrolo M, Nali P. Unified formulation applied to free vibrations finite element analysis of beams with arbitrary section. Shock Vib 2010;17:1–18. http://dx.doi.org/10.3233/SAV-2010-0528.
[52] Carrera E, Petrolo M, Varello A. Advanced beam formulations for free vibration analysis of conventional and joined wings. J Aerospace Eng 2012;25(2). http://dx.doi.org/10.1061/(ASCE)AS.1943-5525.0000130.
[53] Petrolo M, Zappino E, Carrera E. Unified higher-order formulation for the free vibration analysis of one-dimensional structures with compact and bridge-like cross-sections. Thin Wall Struct 2012;56. <http://dx.doi.org/10.1016/j.tws.2012.03.011>.
[54] Ibrahim SM, Carrera E, Petrolo M, Zappino E. Buckling of composite thin walled beams by refined theory. Compos Struct 2012;94(2):563–70.
[55] S.M. Ibrahim, E. Carrera, M. Petrolo, E. Zappino, Buckling of thin walled beams by refined theory, J Zhejiang Univ. Sci A, in press. doi:10.1631/jzus.A1100331.
[56] Carrera E, Petrolo M. Refined beam elements with only displacement variables and plate/shell capabilities. Meccanica 2012;47(3). http://dx.doi.org/10.1007/s11012-011-9466-5.
[57] Carrera E, Petrolo M. Refined one-dimensional formulations for laminated structure analysis. AIAA J 2012;50(1). http://dx.doi.org/10.2514/1.J051219.
[58] Carrera E, Maiaru M, Petrolo M. Component-wise analysis of laminated anisotropic composites. Int J Solids Struct 2012;49(13). <http://dx.doi.org/10.1016/j.ijsolstr.2012.03.025>.
[59] Landahl MT. Kernel function for nonplanar oscillating surfaces in a subsonic flow. AIAA J 1967;5(5):1045–6.
[60] Katz J, Plotkin A. Low-speed aerodynamics: from wing theory to panel methods. New York: McGraw-Hill, Inc.; 1991.
[61] Harder RL, Desmarais RN. Interpolation using surface splines. J Aircr 1972;9(2):189–92.
[62] Demasi L, Livne E. Dynamic aeroelasticity of structurally nonlinear configurations using linear modally reduced aerodynamic generalized forces. AIAA J 2009;47(1).
[63] Varello A, Carrera E, Demasi L. Vortex lattice method coupled with advanced one-dimensional structural models. ASD J 2011;2(2):53–78.
[64] Chen PC. Damping perturbation method for flutter solution: the *g*-method. AIAA J September 2000;38(9):1519–24.
[65] Kameyama M, Fukunaga H. Optimum design of composite plate wings for aeroelastic characteristics using lamination parameters. Comput Struct 2007;85:213–24.
[66] Hollowell SJ, Dugundji J. Aeroelastic flutter and divergence of stiffness coupled, graphite/epoxy cantilevered plates. J Aircr 1984;21(1):69–76.